CURVATURE DUCTILITYOF REINFORCED CONCRETE BEAM SECTIONS STIFFENED WITH STEEL PLATES

Prof. Dr. Thamir K. Al-Azzawi
Dept. of Civil/ College of Engineering
University of Baghdad

Assist. Prof. Raad K. Al Azzawi
Dept. of Civil/ College of Engineering
University of Baghdad

Teghreed H. Ibrahim
Dept. of Civil/ College of Engineering
University of Baghdad

ABSTRCUT

This paper presents theoretical parametric study of the curvature ductility capacity for reinforced concrete beam sections stiffened with steel plates. The study considers the behavior of concrete and reinforcing steel under different strain rates. A computer program has been written to compute the curvature ductility taking into account the spalling in concrete cover. Strain rate sensitive constitutive models of steel and concrete were used for predicting the moment-curvature relationship of reinforced concrete beams at different rate of straining. The study parameters are the yield strength of main reinforcement, yield strength of transverse reinforcement, compressive strength of concrete, spacing of stirrups and steel plate thickness. The results indicated that higher strain rates improve both the curvature ductility and the moment capacity of reinforced concrete beam sections. Moreover the section curvature ductility increases as the thickness of the stiffening plates decreases.

الخلاصة

قدم هذا البحث دراسة نظريه لقابلية مطيلية التقوس لمقاطع الاعتاب الخرسانية المسلحه والمقواة بالصفائح الحديديـــة. تم في هذه الدراسه الأخذ بنظر الأعتبار تصرف كل من الخرسانة وفولاذ التسليح تحت تأثير نســـب قـــيم زمنيـــة مختلفـــة للأنفعال. لحساب مطيلية التقوس تم كتابة برنامج كومبيوتر واخذ بنظر الأعتبار الانفصال الحاصل في غطاء الكونكريت. لقد تم استعمال مخططات متحسسه للمعدل الزمني للأنفعال لكل من الفولاذ والخرسانة وذلك لتوقع علاقة العـــزم مـــع التقـــوس لمقاطع الاعتاب. المتغيرات التي استخدمت في هذه الدراسة هي مقاومة الخضوع لفولاذ التسليح الرئيسي، مقاومة الخضوع لفولاذ التسليح الثانوي، مقاومة الانضغاط للكونكريت، مسافات روابط الاعتاب و سمك صـــفائح الفـــولاذ المقـــواة. النتـــائج المستحصلة من الدراسه أشارت الى أن زيادة المعدلات الزمنية للأنفعال تحسن من المقاومة و قابلية العزم لمقاطع أعتـــاب الكونكريت المسلح. اضافة الى ذلك ازدادت مطيلية التقوس بنقصان سمك صفائح الفولاذ المقواة.

KEYWORDS

Curvature Ductility, Beams, Reinforced Concrete, Steel Plates, Strain Rate.

INTRODUCTION

The philosophy of seismic design for moment resisting reinforced concrete frames is based on the formation of plastic hinges at the critical sections of the frame under the effect of substantial

load reversals in the inelastic range. The ability of the plastic hinge to undergo several cycles of inelastic deformation without significant loss in its strength capacity is usually assessed in terms of the available ductility of the particular reinforced concrete section.

The ductility capacity of reinforced concrete sections is usually expressed in terms of the curvature ductility ratio ($\mu_\phi=\phi_u/\ \phi_y$) where ϕ_y is the curvature of the section at first yield of the tensile reinforcement and ϕ_u is the maximum curvature corresponding to a specific ultimate concrete compression strain.

The moment-curvature analysis of the section is usually performed under monotonically increasing load which represents the first quarter-cycle of the actual hysteretic behavior of the plastic hinge rotation under the earthquake loading. Therefore, μ_ϕ of a section calculated under such assumption is a theoretical estimate of the actual inherent ductility of the section when subjected to an actual earthquake loading. However, the theoretical estimation of μ_ϕ under monotonic loading is widely used as an appropriate indicator of the adequacy of earthquake resistant design for reinforced concrete members.

Steel plates have been used for many years due to their simplicity in applying and their effectiveness for strengthening and stiffening. The high tensile strength and stiffness lead to an increase in bending capacity and a reduction of the deformations. Hussain et. al (1995)[4] tested eight beams of (0.15*0.15*1.25m) with a steel ratio (ρ=0.0096), the concrete cylinder strength was (f_c'=31 MPa) and the average yield strength of the main steel and stirrups was (414 and 275 MPa). The effect of plate thickness and plate end anchorage on ductility and mode of failure of beams were studied and concluded that increasing the plate thickness than 1mm caused a premature failure due to tearing of concrete in the shear span at loads lower than that calculated according to the ACI code shear strength formula.

Soroushian and Sim (1986)[9] used strain rate sensitive constitutive models for steel and concrete to predict the axial load-axial strain relationship of reinforced concrete rectangular columns at different rates of strain. The analysis parameters were the yield strength of reinforcement (f_y =276, 414, 552 MPa), the concrete strength (f_c'=20.7, 27.6 MPa), the steel ratio (ρ=0.026, 0.032, 0.04) and the amounts of hoop reinforcement (ρ_s=0.01388, 0.02082, 0.04164). The results indicated that for the range of analysis parameters considered and for the range of strain rates of (0.00005/sec - 0.5/sec) the secant axial stiffness increases in the range of (16%-36%). Al-Haddad (1995)[1] studied the curvature ductility for reinforced concrete beams under strain rates in a range of (static, 0.05 and 0.1/sec) for values of (f_y =414, 440, 483, 518 MPa) and reinforcement ratio (ρ=0.003, 0.3). He assumed that only the steel reinforcement is a strain rate sensitive. The results indicated that for a strain rate of (0.05/sec) the curvature ductility ratio was decreased by about (12%) for an increase of (34.5 MPa) in f_y compared with that under static loading.

MATERIAL MODELS OF THE PRESENT STUDY

Constitutive Concrete Model

The concrete constitutive model adopted in the present study is that of Razvi & Saatcioglu (1999)[6] which takes into account the cross sectional shape and reinforcement arrangements, **Fig.(1)**. The effect of the strain rate had been accounted for in this model by using the two coefficients (k_f, k_ε) as had been derived by Soroushian (1986)[9] on the test results basis.

The ascending part of the proposed curve is represented by:

$$f_c=\frac{f_{cc}'.k_f.(\frac{\varepsilon_c}{\varepsilon_1.k_\varepsilon}).r}{r-1+(\frac{\varepsilon_c}{\varepsilon_1.k_\varepsilon})^r} \qquad (1)$$

Where: $r=\frac{E_c}{E_c-E_{sec}}$, $E_{sec}=\frac{f_{cc'}.k_f}{\varepsilon_1.k_\varepsilon}$, $E_c=4730\sqrt{f_{c'}}$, $\varepsilon_1=\varepsilon_{01}(1+5k_3K)$

The descending part assumes a slope that changes with confinement reinforcement and as follows:-

$$\varepsilon_{85} = 260 k_3 . \rho_c . \varepsilon_1 [1 + 0.5 k_2 (k_4 - 1)] + \varepsilon_{085} \qquad (2)$$

$$k_1 = 6.7 (f_{le})^{-0.17} \quad , \quad k_2 = 0.15 \sqrt{\left(\frac{b_c}{S}\right)\left(\frac{b_c}{SL}\right)} \le 1 \quad , \quad k_3 = \frac{40}{f_{c'o}} \le 1$$

$$k_4 = \frac{f_{Le}}{500} > 1 \quad , \quad K = \frac{k_1 . f_{Le}}{f_{c'o}}$$

$$\varepsilon_{01} = 0.0028 - 0.008 k_3 \qquad \varepsilon_{085} = \varepsilon_{01} + 0.0018 k_3^2$$

$$\rho_c = \frac{\sum_{i=1}^{n} (A_{sx})_i + \sum_{j=1}^{m} (A_{sy})_j}{S(b_{cx} + b_{cy})}$$

$$f_{Le} = k_2 f_L$$

$$k_f = 1.48 + 0.16 \log_{10} \varepsilon^{\bullet} + 0.0127 (\log_{10} \varepsilon^{\bullet})^2$$

$$k_\varepsilon = 1.08 + 0.112 \log_{10} \varepsilon^{\bullet} + 0.0193 (\log_{10} \varepsilon^{\bullet})^2$$

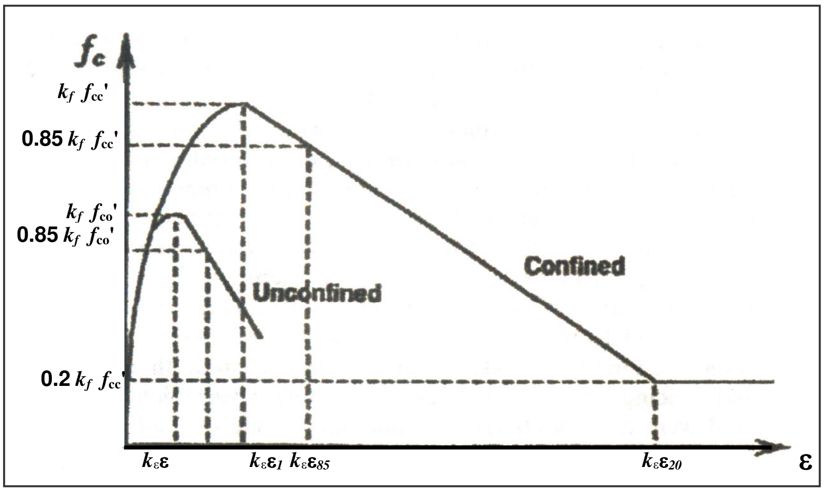

Fig.(1) Strain rate modified stress-strain relationship for concrete[6]

Constitutive Steel Model

Several models were proposed to represent the stress-strain relationship of steel reinforcement by using many dynamic tests results[7]. The following constitutive model of steel has been empirically derived by Parvis Soroushian (1987)[8] from dynamic test results on structural steel, reinforcing bars and deformed wires for different wires and for different types of steel, **Fig.(2)**.

$$f_s = \begin{cases} E_s \varepsilon_s \cdots\cdots & if \quad \varepsilon_s < \dfrac{f_y'}{E_s} \\ f_y' \cdots\cdots & if \quad \dfrac{f_y'}{E_s} < \varepsilon_s < \varepsilon_h' \\ f_y' \left[\dfrac{112(\varepsilon_s - \varepsilon_h') + 2}{60(\varepsilon_s - \varepsilon_h') + 2} + \dfrac{(\varepsilon_s - \varepsilon_h')}{(\varepsilon_u' - \varepsilon_h')} \left(\dfrac{f_u'}{f_y'} - 1.7\right) \right] & if \quad \varepsilon_h' < \varepsilon_s < \varepsilon_u' \\ 0.0 \cdots\cdots & if \quad \varepsilon_s \ge \varepsilon_u' \end{cases} \qquad (3)$$

Where:

$$f_y' = f_y[(-6.54*10^{-8} f_y + 1.46) + (-1.334*10^{-7} f_y + 0.0927)\log_{10} \dot{\varepsilon}] \quad (4)$$

$$f_u' = f_u[(-1.118*10^{-7} f_y + 1.15) + (-0.354*10^{-7} f_y + 0.04969)\log_{10} \dot{\varepsilon}] \quad (5)$$

$$\varepsilon_h' = \varepsilon_h[(-6.105*10^{-6} f_y + 4.46) + (-1.22*10^{-6} f_y + 0.693)\log_{10} \dot{\varepsilon}] \quad (6)$$

$$\varepsilon_u' = \varepsilon_u[(-1.295*10^{-6} f_y + 1.4) + (-2.596*10^{-7} f_y + 0.0827)\log_{10} \dot{\varepsilon}] \quad (7)$$

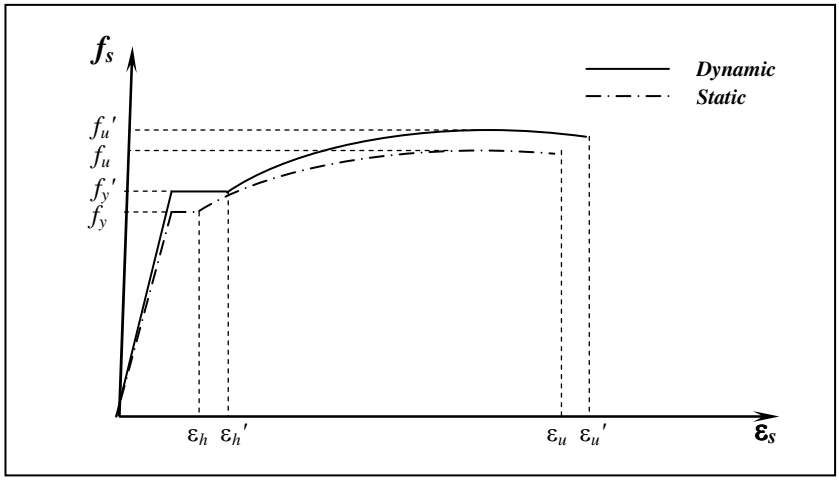

Fig. (2) Comparison of Static and Dynamic Constitutive Model of Steel [8]

The comparison between the experimental (*f*-ε) curve and Parvis Soroushian (1987)[8] constitutive model for two different strain rates for steel specimens with yield strength of (235 MPa) as shown in **Fig.(3).**

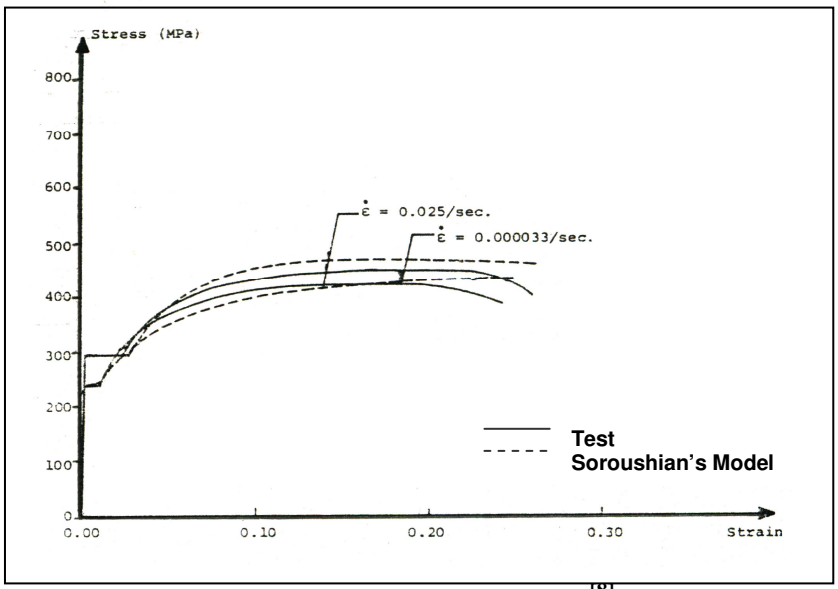

Fig.(3) comparison of Parvis Soroushian (1987) [8] constitutive model of steel with test results for f_y=235 MPa

MOMENT-CURVATURE RELATIONSHIP FOR CONCRETE SECTION

The response of reinforced concrete cross section to an applied bending moment and an axial force may be adequately described by the relation between moment and curvature referred to

moment-curvature relationship. This relation depends on the material and geometrical properties of cross section as well as the level of the applied axial force.
This relationship is established using the following procedure:

1. The ultimate concrete compressive strain is first computed using Bing, Park and Tanka (2001)[2] equation and as follows:

$$\varepsilon_{cu} = \varepsilon_{co}[2 + (122.5 - 0.92 f_{co})\sqrt{\frac{f_l}{f_{co}}}] \quad (8)$$

Where:
f_l =lateral confining stress of transverse reinforcing steel
f_{co} =compressive strength of unconfined concrete
ε_{co}=strain at peak stress of unconfined concrete
The concrete spalling strain is limited by (0.004) as reported in Ref.[5].

2. For a given concrete strain in the extreme compression fiber ε_{cm} and neutral axis depth *kd*, the analysis is performed as follows:
   a) The steel strains (ε_{s1}, ε_{s2}…) can be determined from similar triangles of the strain diagram. For example, for bar *i* at depth d_i the steel strain is:

$$\varepsilon_{si} = \varepsilon_{cm}(\frac{kd - di}{kd}) \quad (9)$$

The steel stresses (f_{s1}, f_{s2}…) corresponding to strains (ε_{s1}, ε_{s2}…) may be found from the stress-strain curve for the steel using equations (3). Then the steel forces (S_{s1}, S_{s2}…) may be found from the steel stresses and the areas of steel, **Fig.(4)**. For example for bar *i* the force equation is:

$$S_i = f_{si} \cdot A_{si} \quad (10)$$

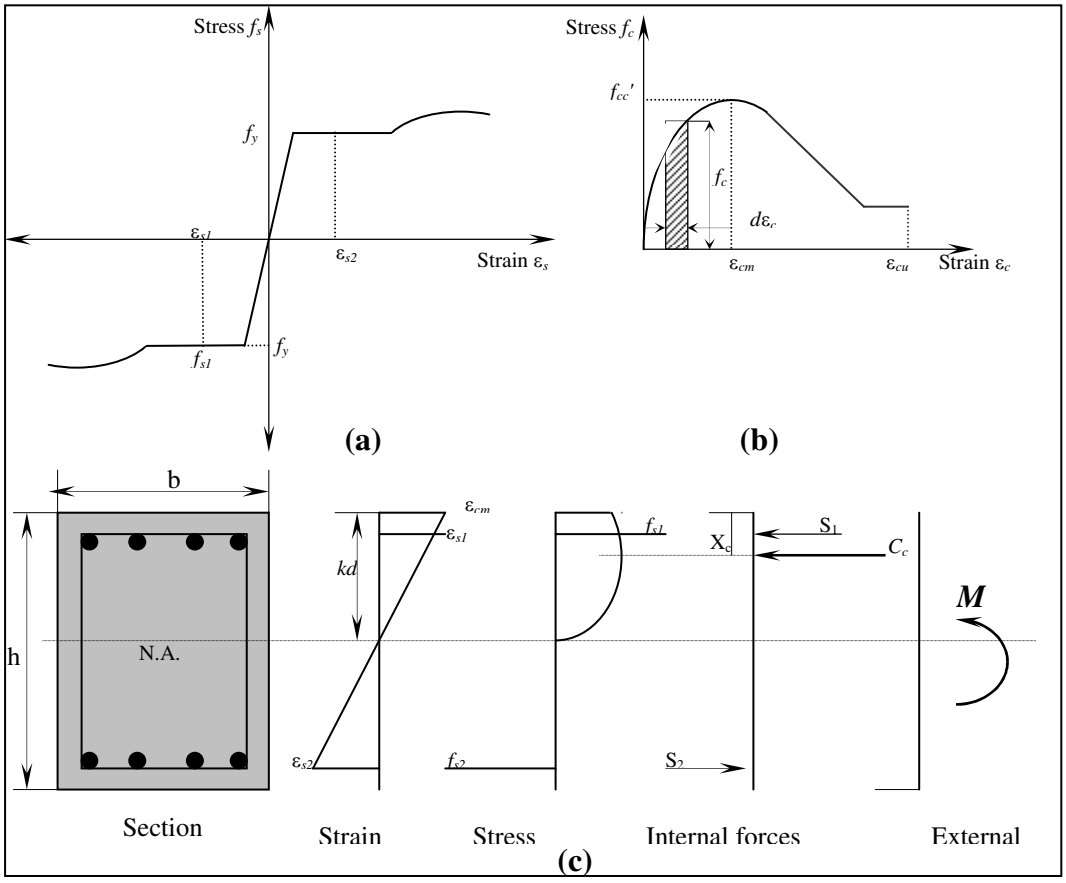

Fig.(4) theoretical moment curvature analysis (a) steel in tension and compression.

b) The concrete compressive force C_c is made up of two parts, a confined part coming from the core concrete confined by the stirrups, and the unconfined part coming from the cover concrete. Each part is analyzed separately and both are added to make up the total concrete compressive force, **Fig.(5)**.

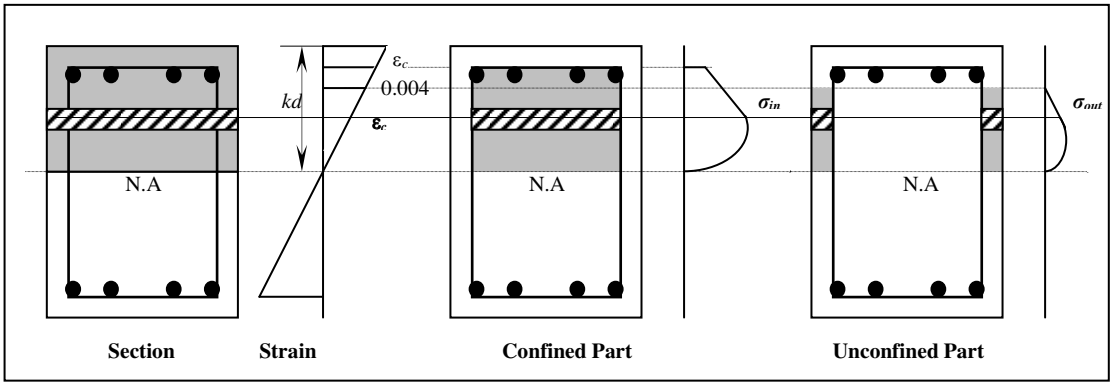

Fig.(5) concrete section analysis.

3. The force equilibrium equation is:

$$C_c = \sum_{i=1}^{n} f_{si} \; A_{si} \qquad (11)$$

and the moment equilibrium equation:

$$M = C_c(\frac{h}{2} - X_c) + \sum_{i=1}^{n} f_{si} \; A_{si}(\frac{h}{2} - d_i) \qquad (12)$$

Where:
X_c=the moment arm of concrete compressive force (C_c).
The curvature is given by

$$\phi = \frac{\varepsilon_{cm}}{kd} \qquad (13)$$

4. The method of establishing these relations is based on equilibrium of internal and external forces assuming a linear distribution of strain across the depth of section. Concrete spalling outside the ties has no contribution in internal force calculation at strains more than the maximum unconfined value of (0.004). The moment-curvature curve exhibits a discontinuity at first yield of tension steel and has been terminated when external fiber compressive concrete strain ε_{cm} reaches the maximum compressive strain ε_{cu}, **Fig.(5)**.

Fig.(6) shows a comparison between experimental results and the present study results. It is obvious that there is a good agreement between the analytical model and the test results.

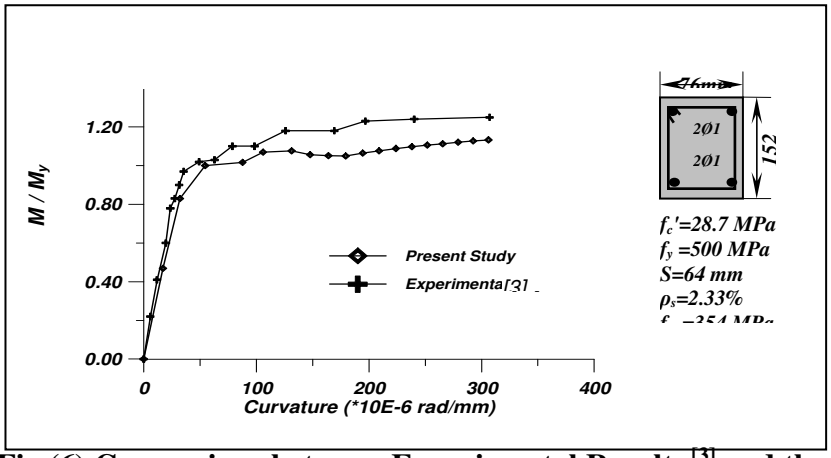

Fig.(6) Comparison between Experimental Results [3] and the Present Studv Results for Confined Beam Section

Effects of Strain Rate on the Curvature Ductility

Any increase in the rate of loading usually increases both the compressive strength of concrete and the yield strength of steel. Hence it may be expected that the moment capacity of reinforced concrete beams increases with increasing in the loading rate.

The reinforced concrete beam shown in **Fig.(7)** is analyzed the results are presented in **Figs.(8)** to **(12)**. In each Figure five curves of moment-curvature relationships are shown for four different strain rates of 0.0001/sec (a typical quasi-static value), 0.001/sec,0.01/sec and 0.1/sec in addition to the static load condition for different parameters of (f_y, f_{yt}, f_c', S and steel plate thickness). The steel plates stiffening the top and the bottom face of the reinforced concrete section.

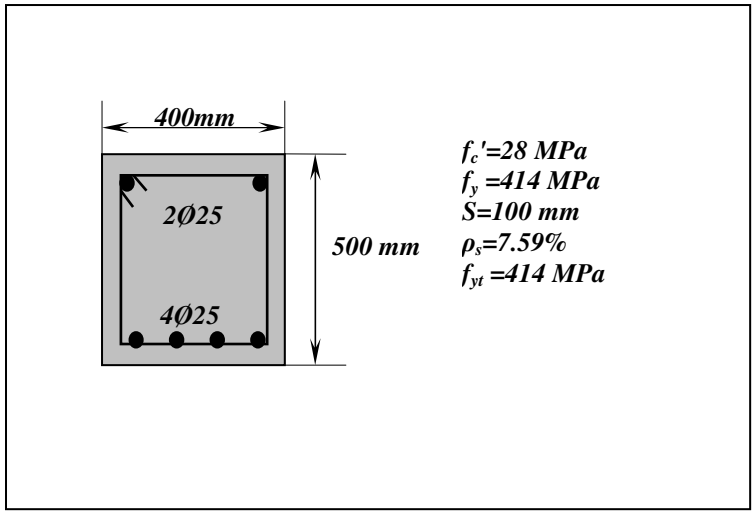

Fig.(7) Details of Beam

Table (1) summarizes the results of the curvature ductility for different parameters (f_y, f_{yt}, f_c' and S). The effects of the above parameters on μ_ϕ for reinforced concrete beam sections are as follows:

1. μ_ϕ is increased by about 10% for f_y =414 MPa and by about 30 % for both f_y =345 and 276 MPa under the strain rate of (0.1/sec) as compared to the static loading, **Fig.(13-a).**
2. For different yield strengths of the transverse reinforcement the curvature ductility factor under the strain rate of (0.1/sec) increased an average by about (14%) as compared to the static loading, **Fig.(13-b)**.

3. For different concrete compressive strengths the average increase in curvature ductility under the strain rate of (0.1/sec) is about (10%) as compared to the static loading, **Fig.(13-c)**.
4. For different values of spacing of stirrups the average increase in μ_ϕ under strain rate of 0.1/sec is about 12% as compared to the static loading**, Fig.(13-d)**.
5. for different f_y, f_c', f_{yt} and S the average increase in moment capacity at strain rate of (0.1/sec) as compared to the static rate is about 20%, **Figs.(8)** to **(11)**.

Effects of Strengthening by Steel Plates

For different strain rates the beam section of **Fig.(7)** has been strengthened by using steel plates of 1mm, 3mm and 5mm thickness. The results are given in **Table (2)** the following can be concluded:

1. For different steel plate thickness the average increase in μ_ϕ under strain rate of 0.1/sec is about 14% as compared to the static loading.
2. For a strain rate of 0.1/sec the strengthening of the beam by steel plates of 1mm, 3mm and 5mm respectively decreases the curvature ductility by 8%, 9% and 10% respectively as compared to the unplated sections.
3. For the static strain rate the strengthening of the beam by steel plates of 1mm, 3mm and 5mm respectively decreases the curvature ductility by 6%, 12% and 18% respectively as compared to the unplated sections.
4. For higher strain rates the increase in thickness of steel plates is become insignificant on the curvature ductility of the beam section, **Fig.(13-e)**.
5. For different steel plate thickness the average increase in moment capacity at strain rate of 0.1/sec over the static rate is (19%), **Fig.(12)**.

Table (1) Curvature ductility μ_ϕ for beams under different strain rates

Strain-Rate (έ) 1/sec	*0. 1*	*0. 01*	*0.001*	*0.0001*	*Static 0.00001*
f_y (MPa)	*f_c'=28 MPa, f_{yt} =414 MPa, S=100mm*				
276	45.28	43.50	40.08	37.16	34.20
345	30.23	30.39	29.05	25.62	22.58
414	18.08	17.53	17.02	16.95	16.28
f_{yt} (MPa)	*f_c'=28 MPa, f_y =414 MPa, S=100mm*				
276	15.58	15.05	14.17	13.86	13.26
345	17.01	16.67	16.17	15.98	14.89
414	18.08	17.53	17.02	16.95	16.28
f_c' (MPa)	*f_y =414 MPa, f_{yt} =414 MPa, S=100mm*				
21	14.39	13.92	13.57	13.32	13.10
28	18.08	17.53	17.02	16.951	16.28
35	19.39	18.90	18.48	18.22	17.47
S(mm)	*f_c'=28 MPa, f_y =414 MPa, f_{yt} =414 MPa*				
100	18.08	17.53	17.02	16.95	16.28
150	13.77	13.14	12.49	12.32	12.01
200	11.82	11.76	11.18	10.88	10.54
250	10.76	10.99	10.37	10.17	9.80

Table (2) Effect of Plate Thickness and Strain Rate on the Curvature Ductility μ_ϕ for Beam Sections

Strain-Rate ($\dot{\varepsilon}$) 1/sec	*0. 1*	*0. 01*	*0.001*	*0.0001*	*Static 0.00001*
Plate Thickness (mm)	*f_c'=28 MPa, f_y =414 MPa, f_{yt} =414 MPa, S=100mm*				
0	18.08	17.53	17.02	16.951	16.28
1	16.75	16.48	15.99	15.94	15.30
3	16.55	16.06	15.89	15.43	14.57
5	16.35	15.86	14.78	14.25	13.81

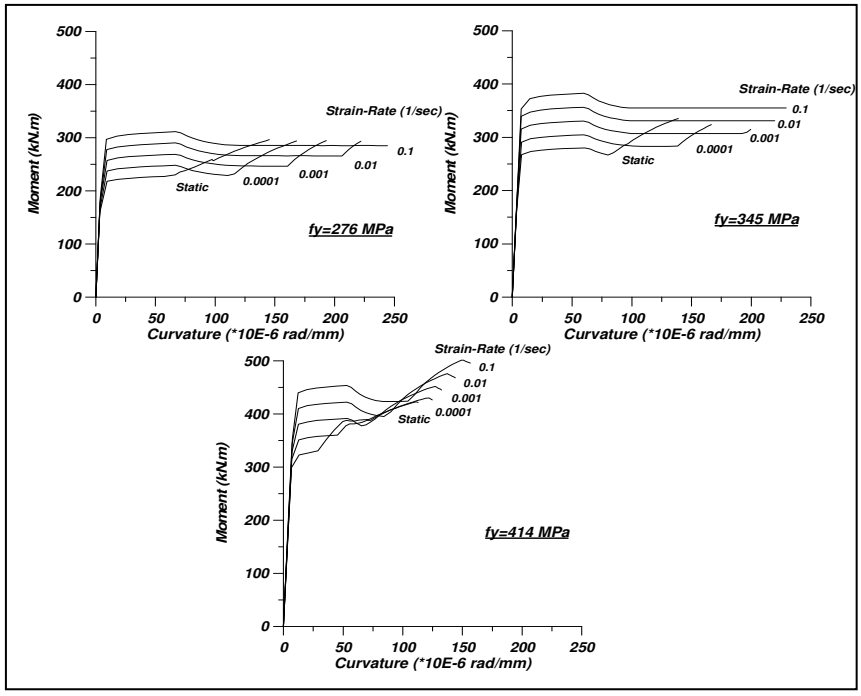

Fig (8) Effect of strain-rate on the moment curvature relationship for different

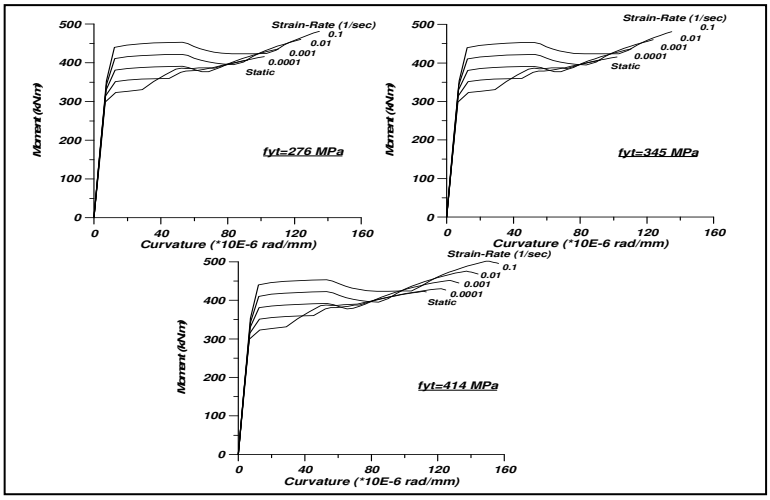

Fig. (9). Effect of strain-rate on the moment curvature

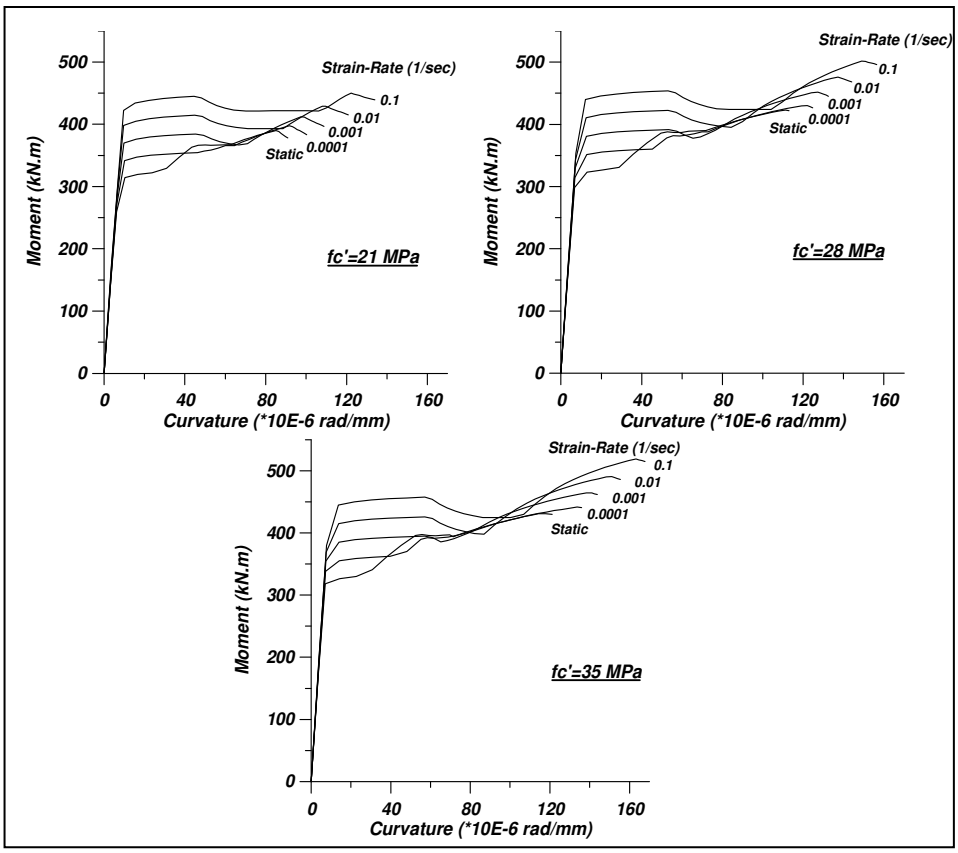

Fig. (10). Effect of strain-rate on the moment curvature relationship for different compressive strength of concrete f_y =414 MPa, f_{yt} =414 MPa, S=100mm

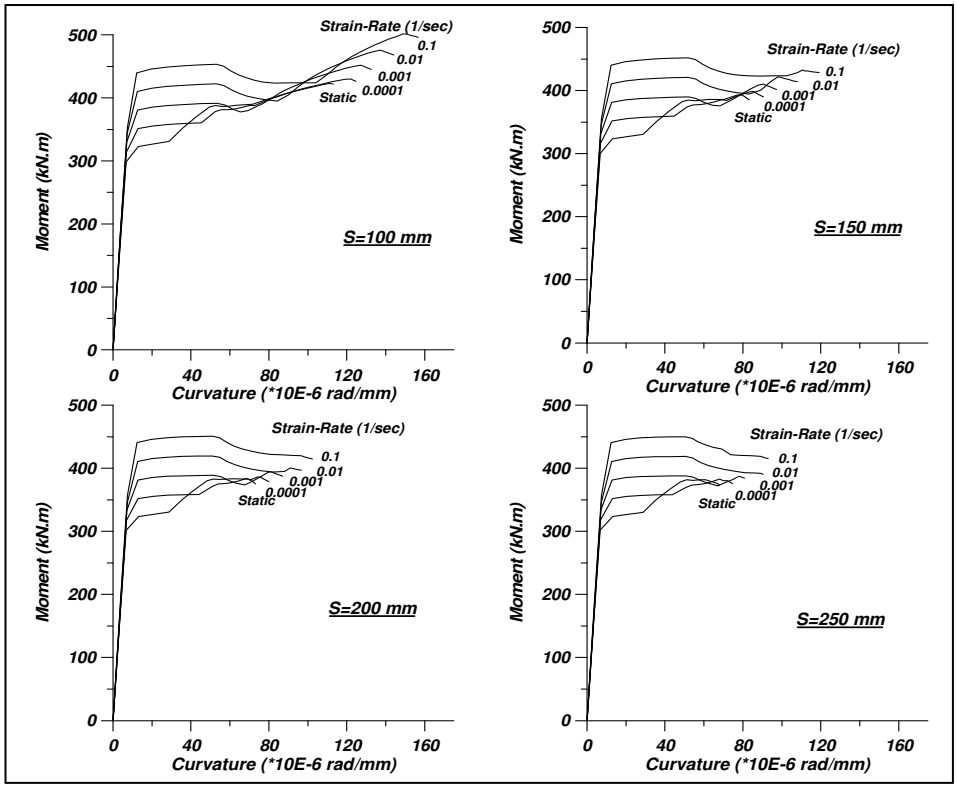

Fig. (11). Effect of strain-rate on the moment curvature relationship for different spacing of transverse reinforcement f_c'=28 MPa, f_y =414 MPa, f_{yt} =414 MPa

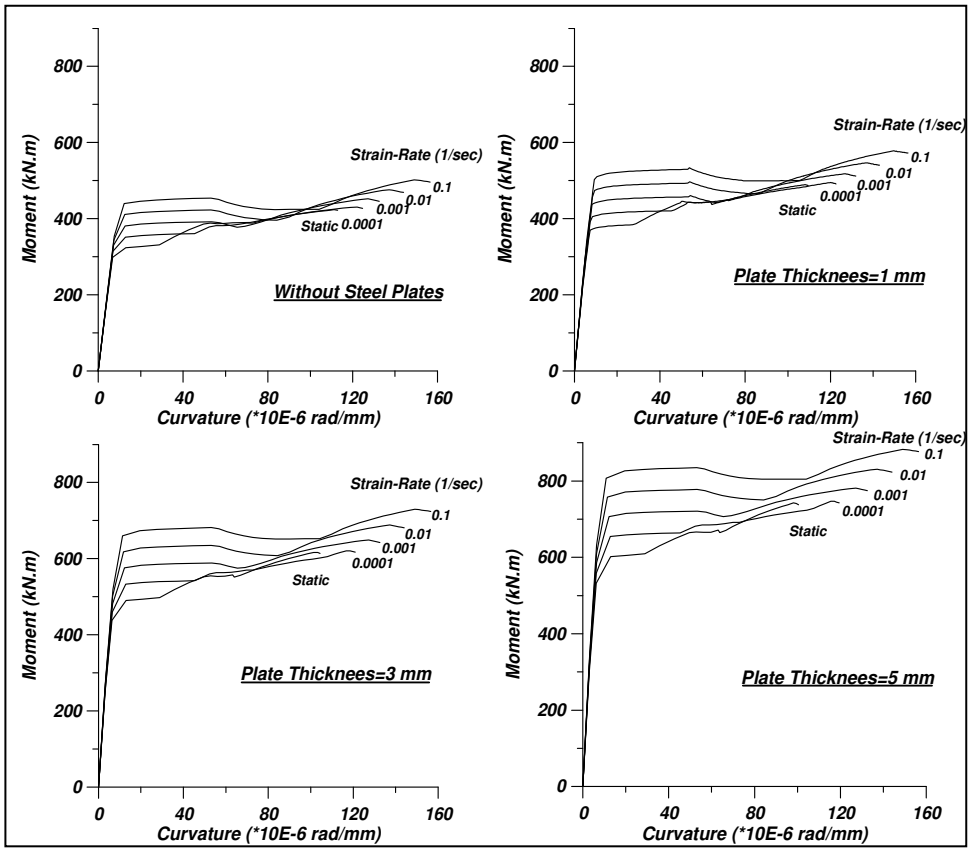

Fig. (12). Effect of strain-rate on the moment curvature relationship for beams with and without steel plates f_c'=28 MPa, f_y =414 MPa, f_{yt} =414 MPa, S=100mm

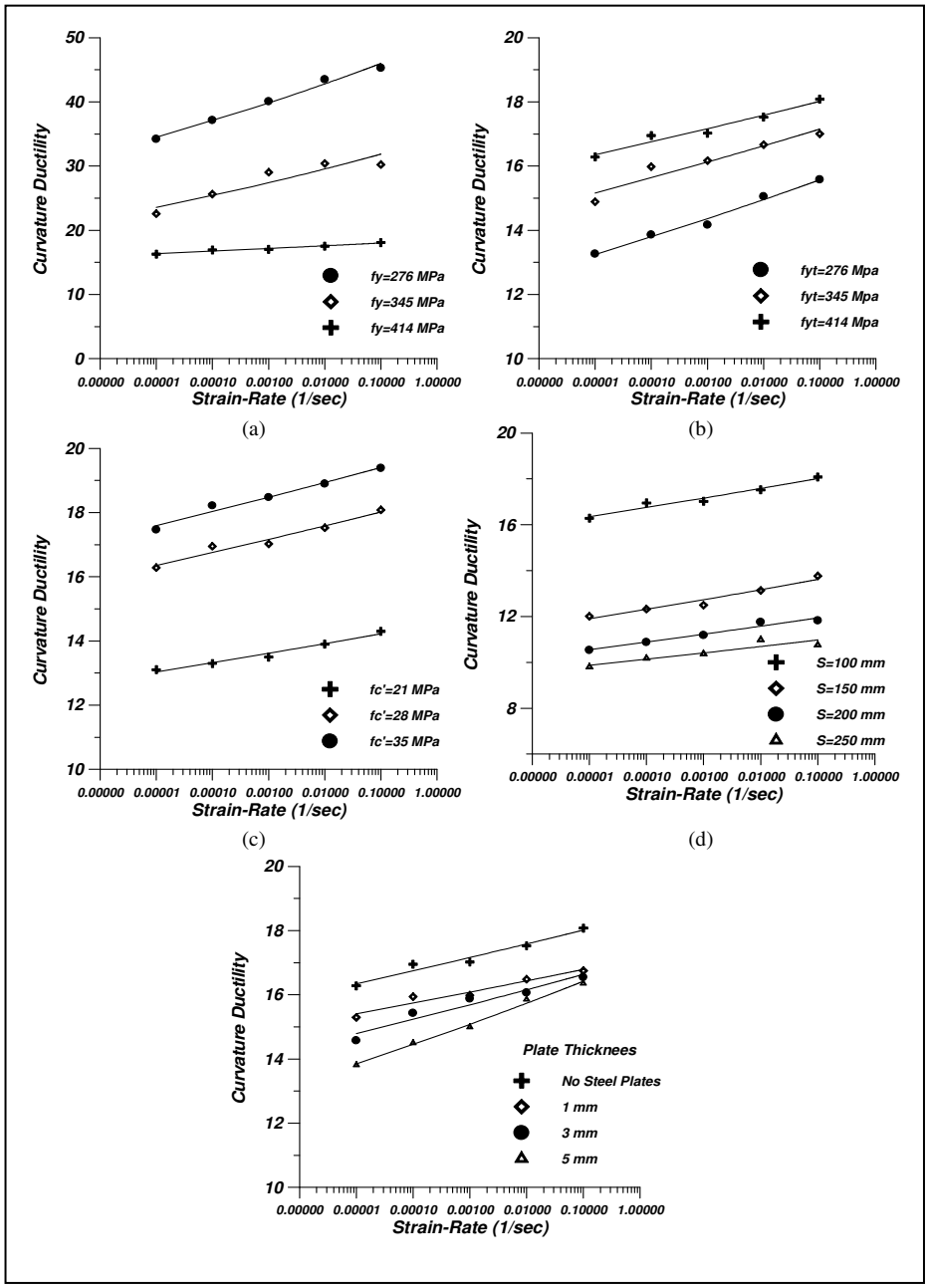

Fig. (13). Effect of strain rate on curvature ductility for different:
(a) Effect of steel yield strength for main reinforcement (f_c'=28 MPa, f_{yt} =414 MPa, S=100mm)
(b) Effect of steel yield strength for transverse reinforcement (f_c'=28 MPa, f_y =414 MPa, S=100mm)
(c) Effect of concrete compressive strength (f_y =414 MPa, f_{yt} =414 MPa, S=100mm)
(d) Effect of spacing of stirrups (f_c'=28 MPa, f_y =414 MPa, f_{yt} =414 MPa)

CONCLUSIONS

Based on the results obtained in the present study, the following conclusions can be drawn:

1. The curvature ductility factor increased by about (14%) for a strain rate of (0.1/sec) as compared to the static loading for different yield strengths of the transverse reinforcement and different steel plate thickness

2. The curvature ductility factor increased on average by (20%) under the strain rate of (0.1/sec) over the static strain rate for different yield strengths of the main reinforcement.
3. The moment capacity increased on average by (20%) for the strain rate of (0.1/sec) as compared to the static load condition for different yield strengths of the main reinforcement, strengths of the transverse reinforcement, compressive strength of concrete, spacing of stirrups and steel plate thickness.
4. The curvature ductility under different strain rates for the sections strengthened by steel plates as compared to the unplated sections decreased for the beam sections by about (10%).

NOTATIONS

A_{sx}, A_{sy}=area of one leg of transverse reinforcement in x and y directions.
b_{cx}, b_{cy}=core dimensions measured c/c of perimeter hoop in x and y directions.
E_c =modulus of elasticity for concrete.
E_s =modulus of elasticity for steel.
E_{sec} =secant modulus of elasticity for concrete.
f_c' = concrete cylinder strength (in MPa).
f_{cc}',f_{co}'= confined & unconfined concrete compressive strength in members (in MPa).
f_L = average confinement pressure (in MPa).
f_{Le}' = equivalent uniform lateral pressure (in MPa).
f_u =static ultimate yield strength of steel (in MPa).
f_u' =dynamic ultimate yield strength of steel (in MPa).
f_y =steel yield strength (in MPa).
f_y' =dynamic yield strength of steel (in MPa).
f_{yt} =yield strength of transverse reinforcement (in MPa).
m, n =number of tie legs in x and y directions.
S =spacing of transverse reinforcement.
S_L =spacing of longitudinal reinforcement laterally supported by corner of hoop or hook of cross tie.
έ =strain rate $\geq 10^{-5}$
ρ_c =total transverse steel area in two orthogonal directions divided by corresponding concrete area.
ε_{01} =strain corresponding to peak stress of unconfined concrete.
ε_{085} =strain corresponding to 85% of peak stress of unconfined concrete on the descending branch.
ε_1 =strain corresponding to peak stress of confined concrete.
ε_{85} =strain corresponding to 85% of peak stress of confined concrete.
ε_c =concrete strain.
ε_h =static strain hardening initiation strains of steel.
ε_h' =dynamic strain hardening initiation strains of steel.
ε_u =static ultimate strains of steel.
ε_u' =dynamic ultimate strains of steel.

REFERENCES

1. Al Haddad, M. S. "Curvature Ductility of R.C. Beams Under Low & High Strain Rates" ACI Structural Jor. , Vol. 92, No. 5, Sep. – Oct. 1995, pp 526 – 534.
2. Bing, L., Park, R. and Tanka, H. “Stress-Strain Behavior of High Strength Concrete Confined by Ultra High and Normal Strength transverse Reinforcements” ACI Str. Journal Vol.98, No.3, May-June 2001, pp. 395–406.
3. Corley, W. G. "Rotational Capacity of Reinforced Concrete Beams" Journal Str. Divi. ASCE Vol. 92, No. st5, October, 1966, pp. 121-146.

4. Hussain, M., Sharif, A., Basunbul, I. A., Baluch, M. H. and Al-Sulaimani, G. J. "Flexural Behavior of Precracked R/C Beams Strengthened Externally by Steel Plates" ACI Str. Journal Vol. 92, No. 1, Jan.–Feb., 1995 pp. 14-22.
5. Park and Paulay “Reinforced Concrete Structures” 1975.
6. Razvi,S. & Saatciaglu ,M. "Confinement Model for High Strength Concrete" Jor. Str. Eng. ASCE, March, 1999.
7. Scott, B. D., Park, R. and Priestley, M. J. N. "Stress-Strain Behavior of Concrete Confined by Overlapping Hoops at Low and High Strain Rates" ACI Jor. January – February, 1982, pp 13 – 27.
8. Soroushian, P. "Steel Mechanical Properties at Different Strain Rates" ASCE Jor. Str. Eng., Vol. 113, No. 4, April, 1987, pp. 663 – 672.
9. Soroushian, P. and Sim, J. "Axial Behavior of R.C. Columns Under Dynamic loads" ACI Jor. November – December 1986, pp 1018 - 1025.